EPJ Web of Conferences **126**, 04018 (2016) DOI: 10.1051/epjconf/201612604018
ICNFP 2015

Production of non-photonic electrons in U+U collisions at $\sqrt{s_{NN}} = 193$ GeV at the STAR experiment

Katarina Gajdosova on behalf of the STAR Collaboration[1,a]

[1] *Czech Technical University in Prague,*
Faculty of Nuclear Sciences and Physical Engineering,
Břehová 7, 115 19 Prague 1, Czech Republic

Abstract. Heavy quarks are suitable probes to study the properties of Quark-Gluon Plasma (QGP), a strongly interacting medium, which can be created in ultrarelativistic heavy-ion collisions at the Relativistic Heavy Ion Collider (RHIC). Non-photonic electrons (NPE) that originate from semileptonic decays of D and B mesons can serve as a good proxy for heavy flavor quarks. Nuclear modification factor R_{AA} of NPE is measured in heavy-ion collisions, which is sensitive to the effect of QGP on heavy quarks.
Measurements of NPE R_{AA} in Au+Au collisions at $\sqrt{s_{NN}} = 200$ GeV reveal that NPE production is strongly suppressed. In year 2012 STAR collected data from U+U collisions at $\sqrt{s_{NN}} = 193$ GeV. In most central collisions higher energy density can be achieved in comparison to collisions of gold nuclei. In this proceedings the preliminary results on NPE in 0-5% most central U+U collisions at a transverse momentum range $1.2 < p_T < 6$ GeV/c are presented. The nuclear modification factor in U+U collisions is compared to that in Au+Au collisions and theoretical models.

1 Introduction

A new state of QCD matter is created during ultrarelativistic heavy-ion collisions at RHIC. One of the suitable probes to study the hot and dense medium, Quark-Gluon Plasma, are heavy quarks charm (c) and bottom (b). Due to their large masses, heavy quarks can be created only in the scatterings with large momenutm transfers which happen during the early stages of heavy-ion collisions before creation of QGP. Thus, their initial production is not affected by this medium, while the final distribution of particles composed of these heavy quarks is modified by the interaction between heavy quarks and QGP and other possible nuclear matter effects.

To quanitfy the effects of nuclear matter vs. the production in p+p collisions we commonly use the nuclear modification factor, R_{AA}. R_{AA} is defined as the ratio of particle production in heavy-ion collisions to particle production in proton-proton collisions scaled by the mean number of binary collisions obtained from Glauber model [1]:

$$R_{AA} = \frac{1}{\langle N_{bin} \rangle} \frac{dN^2_{AA}/dydp_T}{dN^2_{pp}/dydp_T}. \quad (1)$$

[a] e-mail: katka.gajdosova19@gmail.com

If $R_{AA} = 1$, a heavy-ion collision is just a superposition of multiple proton-proton collisions. A so-called suppression is observed when $R_{AA} < 1$, which means that at given p_T and rapidity there are less particles produced in heavy-ion collisions compared to proton-proton collisions due to possible energy loss effects from QGP on heavy quarks.

Heavy quarks have been studied via open heavy flavor measurements. There are two popular approaches to these measurements: direct reconstruction of D mesons via hadronic decay channels, and indirect reconstruction of electrons/muons from semileptonic decays of charm and bottom hadrons. Non-photonic electrons from semileptonic decays of D and B mesons are a good proxy for heavy flavor quarks. Therefore, they are a suitable observable for the study of heavy flavor energy loss mechanisms in QGP. Semileptonic decay channel gained interest due to lower background compared to direct reconstruction in heavy-ion collision environment with thousands of hadrons per event, and the possibility of triggering for high-p_T electrons in electromagnetic calorimeter. The D meson production was measured via the hadronic decay channels in p+p collisions at $\sqrt{s} = 200$ [2] and 500 GeV [3], also in Au+Au collisions at $\sqrt{s_{NN}} = 200$ GeV [4] and U+U collisions at $\sqrt{s_{NN}} = 193$ GeV [3]. The semileptonic decay channels of open heavy flavor have been measured in p+p collisions at $\sqrt{s} = 200$ GeV [5], [6], [7]. Studies of NPE in p+p collisions present an important test of perturbative QCD calculations and are also essential for NPE studies in heavy-ion collisions where they serve as a baseline. The theoretical predictions of FONLL are able to describe the production of NPE and D mesons in p+p collisions well within uncertainties. Modification of NPE spectra in Cu+Cu and Au+Au collisions has been investigated at $\sqrt{s_{NN}} = 200$ GeV [8], [9], [10], [11], [12]. Eventually, it is important to understand the Cold Nuclear Matter effects and be able to distinguish them from QGP effects. Thus, NPE were also studied in d+Au collisions at $\sqrt{s_{NN}} = 200$ GeV [13], [14]. System size dependence of NPE suppression was described in details in [15]. All above mentioned measurements show strong suppression which indicates that heavy quarks lose energy when traversing the QGP.

Uranium nuclei have more nucleons than nuclei of gold. Therefore, by colliding uranium nuclei one can achieve higher energy density than in Au+Au collisions. In Fig. 1 (left) the ratio of energy density of orientation-averaged U+U to Au+Au collisions is plotted as a function of centrality. It is possible to have up to 20% more energy density in uranium nuclei collisions [17]. Therefore, study of NPE production in central U+U collisions with highest energy density achieved at RHIC can reveal whether NPE production will be more suppressed in U+U collisions in comparison to Au+Au collisions at the same centrality class.

2 Detector layout

The Solenoidal Tracker at RHIC (STAR) [16] covers 2π in azimuth and two units of pseudorapidity around mid-rapidity and is wrapped inside a solenoidal magnet, which has a field strength of 0.5 T.

The STAR detector is composed of various subdetectors, each of them fulfilling different task in the particle detection. The detector is shown in Fig. 1 (right).

The main detector of the STAR is the Time Projection Chamber (TPC), which is a gas detector designed for tracking and particle identification using their ionization energy loss in the gas. The Time of Flight (ToF) detector is surrounding the TPC and is able to measure the velocity of particles which improves electron identification at low p_T. The energy of electrons is obtained from the Barrel Electromagnetic Calorimeter (BEMC), which is outside of the ToF. This detector is important in the electron identification at high transverse momentum p_T.

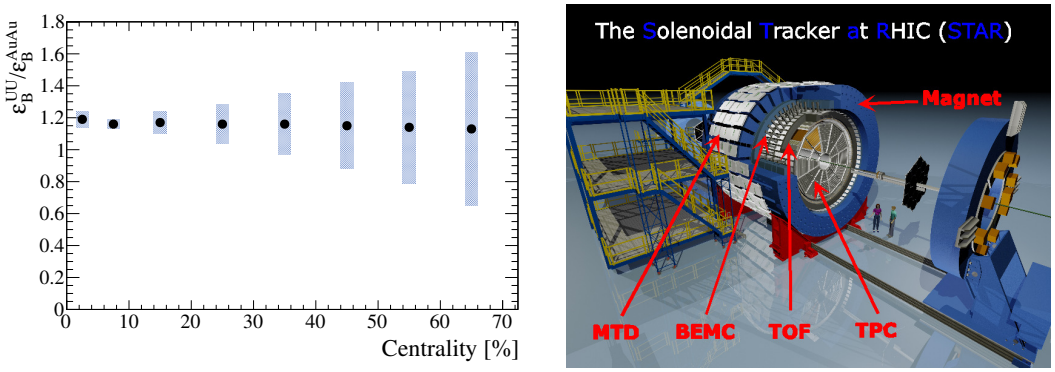

Figure 1: Left: Ratio of energy densities in U+U and Au+Au collisions as a function of centrality. Taken from Ref. [17]. Right: View of the STAR detector.

3 Analysis procedure

The data sample used for the analysis presented in this proceedings comes from 0-5% most central U+U collisions at $\sqrt{s_{NN}}$ = 193 GeV taken during the year 2012 (run12) at the STAR experiment. The total number of events was 40 M. In this analysis the TPC and BEMC detectors were used for particle identification, tracking and extraction of energy information. The centrality was selected based on ToF and Zero Degree Calorimeter (ZDC) detectors.

As was already mentioned above, non-photonic electrons originate in semileptonic decays of open heavy flavor mesons. It is not possible to reconstruct the invariant mass of $D(B)$ meson due to missing neutrino from the decay, so we measure a continuous spectrum. This measurement is accompanied by large background caused by photonic electrons, which are always created in pairs e^+e^- and mainly come from photon conversions $\gamma \rightarrow e^+ + e^-$ and Dalitz decays of η and π^0. This background has to be subtraced from the electron sample. Thus, the non-photonic electron yield is obtained according the following formula

$$N_{npe} = N_{inclusive}\epsilon_{purity} - N_{photonic}/\epsilon_{photonic}, \tag{2}$$

where N_{inc} is the inclusive electron candidate yield, ϵ_{purity} is the purity of the inclusive electron sample, $N_{photonic}$ is the photonic electron yield and $\epsilon_{photonic}$ is the photonic electron reconstruction efficiency. First, the inclusive electron sample is obtained using selection criteria from TPC and BEMC detectors and corrected with the purity for hadron contamination. Then, the photonic electrons are subtracted. We cannot detect all photonic electrons pairs. Therefore, the photonic electron yield needs to be corrected for the photonic electron reconstruction efficiency.

The purity of inclusive electron sample is calculated from the normalized electron energy loss distribution $n\sigma_e$ in TPC which is fitted with multi-Gaussian function at various p_T bins. Figure 2 (left) shows $n\sigma_e$ distribution for the p_T bin $2.0 < p_T < 3.0$ GeV/c. Due to large remaining hadron contamination, the multi-Gaussian function is used. The purity is then defined as the ratio of integral under electron Gaussian to the multi-Gaussian within the $n\sigma_e$ cut. The inclusive electron sample in this analysis is rather clean with ϵ_{purity} almost equal unity due to tight cut on $n\sigma_e$, constant over transverse momentum range: $-0.5 < n\sigma_e < 2.5$ (also plotted in Fig. 2 (left) with dark green lines)

In Fig. 2 (right) the invariant mass of electron pairs with trigger electrons at $2.0 < p_T < 3.0$ GeV/c is shown. Electrons are paired with each other and grouped together according to their charges.

The unlike-sign distribution (blue color) represents all e^+e^- pairs while like-sign distribution (red color) characterises the combinatorial background which is subtracted from the unlike-sign pairs. The resulting distribution - unlike-like sign (black color) - contains the real photonic electron pairs. As can be seen in Fig. 2 (right): only at low m_{ee} there are entries reflecting the low invariant mass of γ or π^0, η.

The photonic electron reconstruction efficiency is calculated with Monte Carlo (MC) simulation. First, particle tracks are generated which originate at a collision vertex. These simulated tracks are embedded into a real collision and propagated through the detector using GEANT, simulating the detector response for each particle. The simulation data are then reconstructed using the same reconstruction chain used in real data reconstruction. Final photonic electron reconstruction efficiency varies from 30% at low p_T to 50% at high p_T.

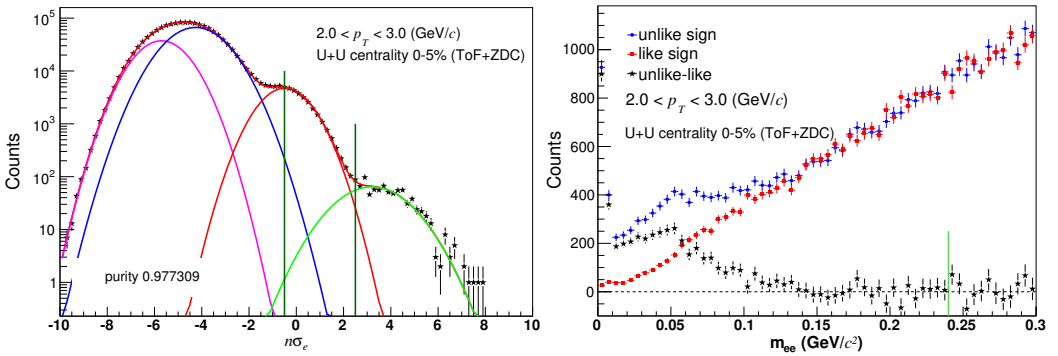

Figure 2: Left: Distribution of standard ionization energy loss in the TPC. Each particle contribution is denoted in different colors. The blue line represents π, the pink line $K + p$, the red line are electrons, and finally the green line are the so called merged pions which wrongly reconstruct two tracks as one. Right: Invariant mass of electron pairs.

3.1 Invariant yield of non-photonic electrons

The invariant yield of non-photonic electrons is calculated as follows:

$$\frac{1}{2\pi p_T}\frac{d^2N}{dp_T d\eta} = \frac{1}{2}\frac{1}{2\pi p_T}\frac{1}{\Delta p_T}\frac{1}{\Delta\eta}\frac{N_{npe}}{N_{events}}\frac{1}{\epsilon_{bemc}\epsilon_{n\sigma_e}\epsilon_{trk}}, \tag{3}$$

where N_{events} is total number of events of data sample used for this analysis, and ϵ_{bemc}, $\epsilon_{n\sigma_e}$ and ϵ_{rec} are the different efficiency components in the analysis. ϵ_{emc} is the efficiency of electron identification cuts using BEMC detector which goes from 30% at low p_T up to 70% at high p_T. $\epsilon_{n\sigma_e}$ is the efficiency of electron identification using energy loss in TPC and is about 50% through the whole p_T range used in this analysis. Finally, ϵ_{trk} is the efficiency of single track reconstruction in TPC. Monte Carlo simulations were used to calculate this efficiency too and the result is about 40%.

Invariant yield of non-photonic electrons is shown in Fig. 3 in a transverse momentum range $1.2 < p_T < 6.0$ GeV/c. The background contribution from J/ψ decays was estimated and subtracted from the NPE yield. Blue lines represent statistical uncertainties and blue boxes show systematical

uncertainties. The main sources of systematic uncertainties are estimation of photonic electron reconstruction efficiency, purity estimation, and calculation of BEMC efficiency ϵ_{bemc}, $\epsilon_{n\sigma_e}$ and single track reconstruction efficiency ϵ_{trk}. The largest source is from BEMC efficiency ϵ_{bemc}, while the lowest one is from ϵ_{trk}.

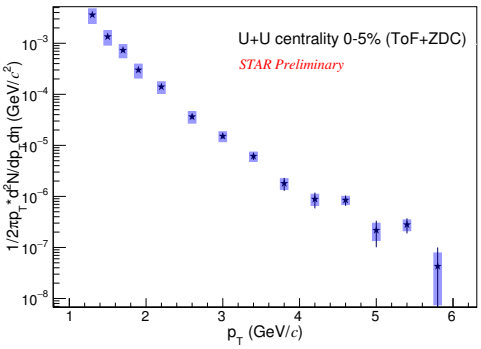

Figure 3: Invariant yield of non-photonic electrons as a function of p_T in 0-5% most central U+U collisions at $\sqrt{s_{NN}}$ = 193 GeV.

4 Nuclear modification factor

Invariant yield of NPE in U+U collisions was scaled by the mean number of binary collisions N_{bin} = 1156 ± 163 for 0-5% most central events and divided by the NPE yield in p+p collisions taken during the year 2012 at the STAR experiment [18]. The nuclear modification factor of NPE in 0-5% most central U+U collisions in 1.2 < p_T < 6.0 is plotted in Fig. 4 (left). It is consistent with 1 for p_T < 2.5 GeV/c and reveals strong suppression for p_T > 2.5 GeV/c. Yield of NPE in Au+Au collisions [18] was obtained in the same way as the one in U+U collisions and the same p+p reference was used. Nuclear modification factor of NPE in U+U collisions is consistent within errors but there is indication of lower R_{AA} than in Au+Au collisions. R_{AA} of NPE in U+U collisions is compared to theoretical model including CNM effects (Cronin effect and initial state energy loss), QGP effects such as jet quenching, and new attenuation mechanism for open heavy flavor mesons, called collisional dissociation, originating from short formation times of D and B mesons. The dashed green line represents the case with lower initial state energy loss but large Cronin effect and the dot-dashed magenta line the case with higher initial state energy loss and small Cronin effect [19], [20], [21].

In addition, nuclear modification factor of NPE as a function of number of participants is plotted in Fig. 4 (right). R_{AA} of NPE in U+U and Au+Au collisions are plotted with blue and red closed symbols, respectively. The statistical uncertainties are represented by the vertical lines and systematical uncertainties are shown by the filled boxes. R_{AA} in U+U collisions extends the trend in Au+Au collisions and the overall suppression is similar within uncertainties to the one of D meson [4] and light hadrons [22].

5 Summary

In summary, first preliminary results of non-photonic electrons in 0-5% most central U+U collisions at the STAR experiment were shown in this proceedings. The nuclear modification factor of NPE

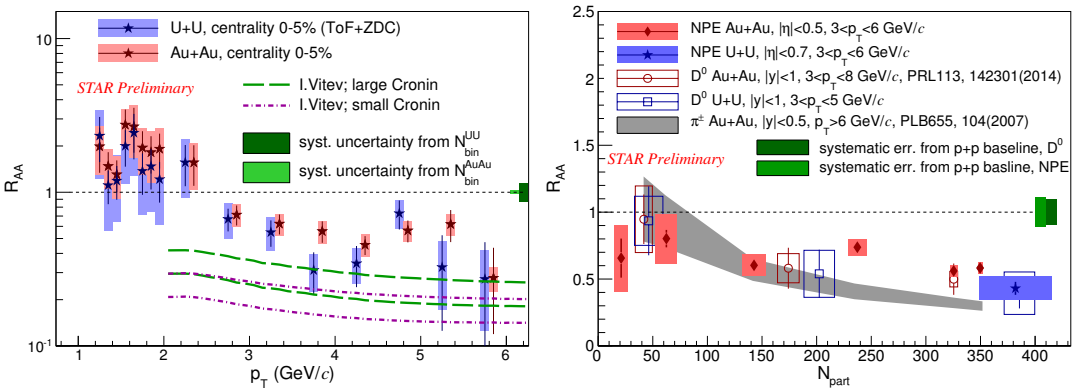

Figure 4: Left: Nuclear modification factor of NPE versus p_T in U+U collisions compared to AuAu collisions and model [19], [20], [21]. Right: Nuclear modification factor of NPE in U+U and Au+Au collisions, D mesons in U+U and Au+Au collisions [4] and $\pi^{\pm}$ in Au+Au collisions [22] versus number of participants.

in U+U collisions was shown in transverse momentum range $1.2 < p_T < 6.0$ GeV/c and was also compared to R_{AA} in Au+Au collisions and model including CNM effects, QGP effects and collisional dissociation. R_{AA} of NPE in U+U collisions is similar within uncertainties, but there is indication of lower R_{AA} than that in Au+Au collisions at the same centrality class. Also, R_{AA} of NPE versus mean number of participants was shown. The nuclear modification factor of NPE in U+U collisions extends the trend of that in Au+Au collisions. R_{AA} of NPE was also compared to the one of D mesons measured via hadronic decay channel and R_{AA} of light hadrons. The magnitude of suppression is similar within uncertainties.

Acknowledgements

This work was supported by Grant Agency of the Czech Technical University in Prague, grant No. SGS13/215/OHK4/35/14 and by Grant Agency of the Czech Republic, grant No. 13-20841S.

References

[1] M. L. Miller *et al.*, Ann. Rev. Nucl. Part. Sci. **57**, 205 (2007).
[2] L. Adamczyk *et al.* (STAR Collaboration), Phys. Rev. D **86**, 072013 (2012).
[3] Z. Ye for the STAR Collaboration, Quark Matter proceedings, Nucl. Phys. A **931**, 520 (2014).
[4] L. Adamczyk *et al.* (STAR Collaboration), Phys. Rev. Lett. **113**, 142301 (2014).
[5] H. Agakishiev *et al.* (STAR Collaboration), Phys. Rev. D **83**, 052006 (2011).
[6] A. Adare *et al.* (PHENIX Collaboration), Phys. Rev. Lett. **97**, 252002 (2006).
[7] A. Adare *et al.* (PHENIX Collaboration), Phys. Rev. Lett. **96**, 032001 (2006).
[8] A. Adare *et al.* (PHENIX Collaboration), Phys. Rev. C **86**, 024909 (2012).
[9] B. I. Abelev *et al.* (STAR Collaboration), Phys. Rev. Lett. **98**, 19301 (2007); Erratu m-ibid. **106**, 159902 (2011).

[10] A. Adare *et al.* (PHENIX Collaboration), Phys. Rev. Lett. **98**, 172301 (2007).
[11] A. Adare *et al.* (PHENIX Collaboraton), Phys. Rev. C **84**, 044905 (2010).
[12] A. Adare *et al.* (PHENIX Collaboration), arXiv:1509.04662 [nucl-ex] (2015).
[13] A. Adare *et al.* (PHENIX Collaboration), Phys. Rev. Lett. **109**, 242301 (2012).
[14] A. Adare *et al.* (PHENIX Collaboration), Phys. Rev. Lett. **112**, 252301 (2014).
[15] A. Adare *et al.* (PHENIX Collaboration), Phys. Rev. C **90**, 034903 (2014).
[16] K.H. Ackermann *et al.*, Nucl. Instrum. Meth. **A 499**, 624 (2003).
[17] D. Kikola, G. Odyniec, R. Vogt, Phys. Rev. C **84**, 054907 (2011).
[18] X. Bai for the STAR Collaboration, poster contribution at Quark Matter 2015.
[19] R. Sharma, I. Vitev, B.-W. Zhang, Phys. Rev. C **80**, 054902 (2009).
[20] R. Sharma, I. Vitev, Phys. Rev. C **87**, 044905 (2013).
[21] Z.-B. Kang *et al.*, Phys. Rev. Lett. **114**, 092002 (2015).
[22] B. I. Abelev *et al.* (STAR Collaboration), Phys. Lett. B **655**, 104 (2007).